Supporting information

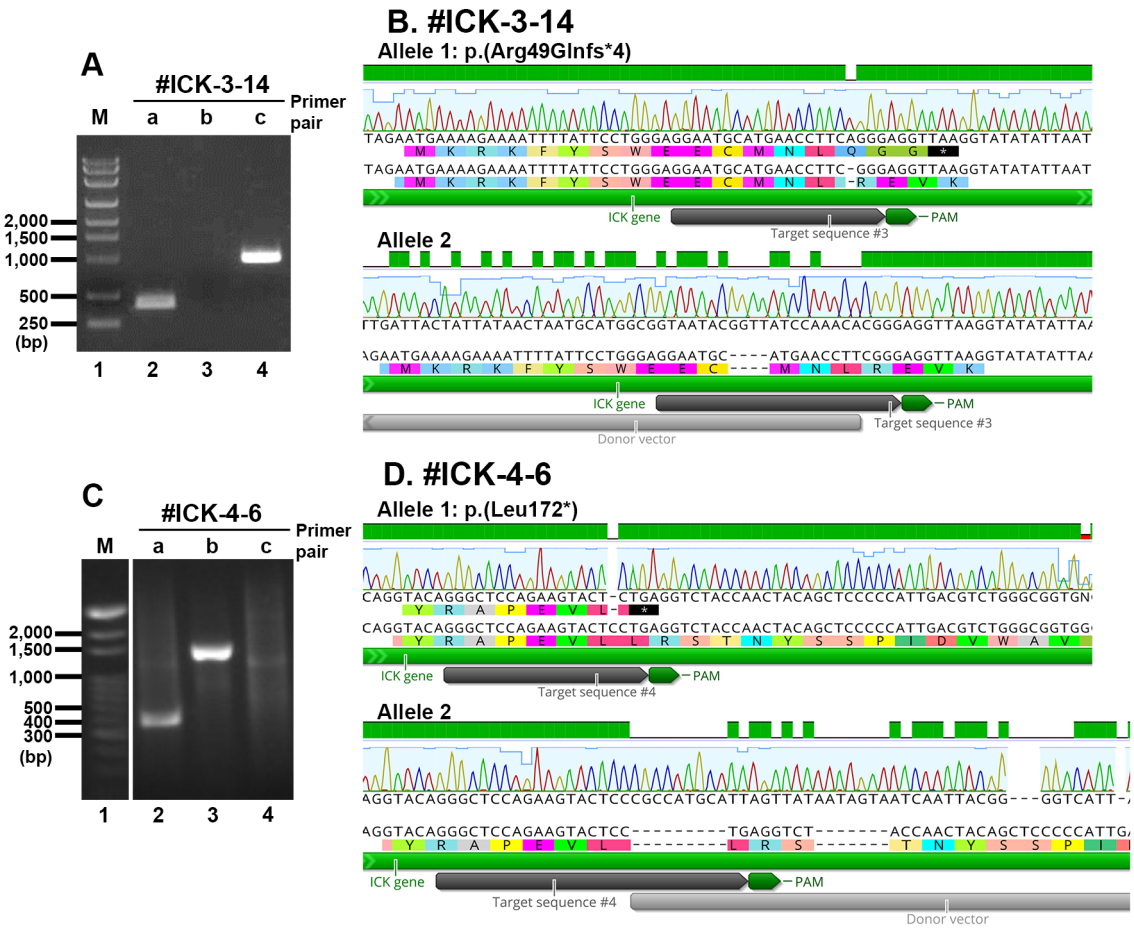

Fig. S1. Genomic PCR and sequence analyses of the *ICK*-KO cell lines

(A, C) Genomic DNA extracted from the *ICK*-KO cell lines #ICK-3-14 (A) and #ICK-4-6 (C), which were established using a donor knock-in vector containing distinct target sequences, were subjected to PCR analysis using the indicated primer sets (see Table S2, #3 and #4) to detect alleles with a small indel or no insertion (a), or with forward (b) or reverse (c) integration of the donor knock-in vector. M, molecular weight markers (A, pPSU1+ ladder; C, PSU 100bp ladder). (B and D) Alignments of allele sequences of the #ICK-3-14 (B) and #ICK-4-6 (D) cell lines determined by sequencing of the PCR products shown in (A) and (C). Positions of the target sequence and PAM sequence, and insertion sites of the donor knock-in vector are indicated.

Table S1. Plasmids used in this study

Vector	Insert	Reference
pCAG-EGFP-C	ICK	This study
pCAG-EGFP-C	ICK(1–287)	This study
pCAG-EGFP-C	ICK(285–632)	This study
pCAG-EGFP-C	ICK(285–561)	This study
pCAG-EGFP-C	ICK(285–537)	This study
pCAG-EGFP-C	ICK(285–501)	This study
pCAG-EGFP-C	ICK(285–473)	This study
pCAG-EGFP-C	ICK(285–361)	This study
pmCherry-C	IFT22	(Takei *et al.*, 2016)
pmCherry-C	IFT25	This study
pmCherry-C	IFT27	This study
pmCherry-N	IFT20	This study
pCAG2-mCherry-C	IFT38	This study
pmCherry-C	IFT54	This study
pCAG-mCherry-C	IFT57	(Nozaki *et al.*, 2019)
pCAG-mCherry-C	IFT46	(Katoh *et al.*, 2016)
pCAG-mCherry-C	IFT52	(Katoh *et al.*, 2016)
pCAG2-mCherry-C	IFT56	This study
pCAG-mCherry-C	IFT70A	(Takei *et al.*, 2016)
pCAG-mCherry-C	IFT88	(Katoh *et al.*, 2016)
pCAG-mCherry-C	IFT74	(Katoh *et al.*, 2016)
pCAG-mCherry-C	IFT81	(Katoh *et al.*, 2016)
pCAG-mCherry-N	IFT80	(Katoh *et al.*, 2016)
pCAG2-mCherry-C	IFT172	(Katoh *et al.*, 2016)
pCAG2-mCherry-C	IFT43	(Hirano *et al.*, 2017)
pCAG2-mCherry-C	IFT121	(Hirano *et al.*, 2017)
pCAG2-mCherry-C	IFT122	(Hirano *et al.*, 2017)
pCAG2-mCherry-C	IFT139	(Hirano *et al.*, 2017)
pCAG2-mCherry-C	IFT140	(Hirano *et al.*, 2017)
pCAG2-mCherry-C	IFT144	(Hirano *et al.*, 2017)
pRRLsinPPT-mCherry-C-IRES-Blast	ICK	This study

pRRLsinPPT-mCherry-C-IRES-Blast	ICK(1–287)	This study
pRRLsinPPT-mCherry-C-IRES-Blast	ICK(285–632)	This study
pRRLsinPPT-mCherry-C-IRES-Blast	ICK(285-561)	This study
pRRLsinPPT-mCherry-C-IRES-Blast	ICK(285–537)	This study
pRRLsinPPT-mCherry-C-IRES-Blast	ICK(285–501)	This study
pRRLsinPPT-mCherry-C-IRES-Blast	ICK(285–473)	This study
pRRLsinPPT-mCherry-C-IRES-Blast	ICK(K33R)	This study
pRRLsinPPT-mCherry-C-IRES-Blast	ICK(T157A)	This study
pRRLsinPPT-mCherry-C-IRES-Blast	ICK(T157E)	This study
pRRLsinPPT-mCherry-C-IRES-Blast	–	This study
pRRLsinPPT-mCherry-C-IRES-Blast	IFT88	This study
pRRLsinPPT-EGFP-N-IRES-Zeo	ARL13B(ΔGD; 1–19, 190–428 aa)	This study
pDonor-tBFP-NLS-Neo (Universal)	–	(Katoh *et al.*, 2017)
peSpCas9 (1.1)-2×gRNA	–	(Katoh *et al.*, 2017)
pGEX-6P1	anti-GFP Nb	(Katoh *et al.*, 2015)

Notes: All cDNA inserts except for that of anti-GFP Nb are of human origin.

Table S2. Antibodies used in this study

Antibody	Manufacturer or provider	Clone/catalog number or reference	Dilution (purpose)
Polyclonal rabbit anti-IFT88	Proteintech	13967-1-AP	1:1,000 (IF, IB)
Polyclonal rabbit anti-IFT70	Proteintech	25352-1-AP	1:1,000 (IB)
Polyclonal rabbit anti-IFT139	Sigma-Aldrich	HPA035495	1:1,000 (IB)
Polyclonal rabbit anti-IFT140	Proteintech	17460-1-AP	1:500 (IF)
Polyclonal rabbit anti-GPR161	Proteintech	13398-1-AP	1:200 (IF)
Polyclonal rabbit anti-ARL13B	Proteintech	17711-1-AP	1:1,000 (IF)
Monoclonal mouse anti-ARL13B	Abcam	N29566	1:500 (IF)
Monoclonal mouse anti-SMO	Santa Cruz	sc-166685	1:100 (IF)
Monoclonal mouse anti-FOP	Abnova	2B1	1:5,000 (IF)
Monoclonal mouse anti-Ac-α-tubulin	Sigma-Aldrich	6-11B-1	1:1,000 (IF)
Monoclonal mouse anti-RFP	MBL	3G5	1:1,000 (IF)
Monoclonal mouse anti-GFP	Proteintech	66002-1-Ig	1:5,000 (IB)
Polyclonal rabbit anti-RFP	Proteintech	26765-1-AP	1:5,000 (IB)
Monoclonal mouse anti-GFP	BD Biosciences	JL-8	1:1,000 (IB)
Monoclonal mouse anti-β-tubulin	Proteintech	66240-1-Ig	1:10,000 (IB)
AlexaFluor-conjugated secondary	Molecular Probes	A11034, A21121, A21127, A21137, A21242	1:1,000 (IF)
Peroxidase-conjugated secondary	Jackson ImmunoResearch	115-035-166, 111-035-144	1:3,000 (IB)

Notes: IF, immunofluorescence; IB, immunoblotting

Table S3: Oligo DNAs used in this study

Name	Sequence
pTagBFP-N-RV2 (primer 3)	5'-CGTAGAGGAAGCTAGTAGCCAGG-3'
ICK-genome#3-FW (primer 1)	5'-ACAGCAGTCCAGGCCTCTTTG-3'
ICK-genome#3-RV (primer 2)	5'-TGCCTCCCTTTCCAGCATTAGTG-3'
ICK-genome#4-FW (primer 4)	5'-TTGTCAACAGCAGCCCACGG-3'
ICK-genome#4-RV (primer 5)	5'-AGTGCTGAACAGGGCTGAGC-3'
ICK-gRNA#3-S	5'- CACCGGAATGCATGAACCTTCGGG-3'
ICK-gRNA#3-AS	5'-AAACCCCGAAGGTTCATGCATTCC-3'
ICK-gRNA#4-S	5'-CACCGGGCTCCAGAAGTACTCCTG-3'
ICK-gRNA#4-AS	5'-AAACCAGGAGTACTTCTGGAGCCC-3'

Video S1. ECV formation from cells shown in Fig. 5C

The *ICK*-KO cell line (#ICK-4-6) stably expressing ARL13B(ΔGD)-EGFP was processed for live cell imaging as described in Experimental Procedures.

Video S2. ECV formation from cells shown in Fig. 5D

The *ICK*-KO cell line (#ICK-4-6) stably expressing ARL13B(ΔGD)-EGFP was processed for live cell imaging as described in Experimental Procedures.

Video S3. ECV formation from cells shown in Fig. 5E

The *ICK*-KO cell line (#ICK-4-6) stably expressing ARL13B(ΔGD)-EGFP was processed for live cell imaging as described in Experimental Procedures. Note that this video shows the release of ECVs from the cilia of two independent cells.

Video S4. ECV formation from cells shown in Fig. 5F

The *ICK*-KO cell line (#ICK-4-6) stably coexpressing ARL13B(ΔGD)-EGFP and mChe-IFT88 was processed for live cell imaging as described in Experimental Procedures.

Video S5. Bidirectional movement of ICK-positive particles within cilia

The *ICK*-KO cell line (#ICK-4-6) stably coexpressing mChe-ICK(WT) was processed for TIRF microscopy as described in Experimental Procedures.

Supporting references

Hirano, T., Katoh, Y., and Nakayama, K. (2017). Intraflagellar transport-A complex mediates ciliary entry as well as retrograde trafficking of ciliary G protein-coupled receptors. Mol. Biol. Cell *28*, 429-439.

Katoh, Y., Michisaka, S., Nozaki, S., Funabashi, T., Hirano, T., Takei, R., and Nakayama, K. (2017). Practical method for targeted disruption of cilia-related genes by using CRISPR/Cas9-mediated homology-independent knock-in system. Mol. Biol. Cell *28*, 898-906.

Katoh, Y., Nozaki, S., Hartanto, D., Miyano, R., and Nakayama, K. (2015). Architectures of multisubunit complexes revealed by a visible immunoprecipitation assay using fluorescent fusion proteins. J. Cell Sci. *128*, 2351-2362.

Katoh, Y., Terada, M., Nishijima, Y., Takei, R., Nozaki, S., Hamada, H., and Nakayama, K. (2016). Overall architecture of the intraflagellar transport (IFT)-B complex containing Cluap1/IFT38 as an essential component of the IFT-B peripheral subcomplex. J. Biol. Chem. *291*, 10962-10975.

Nozaki, S., Castro Araya, R.F., Katoh, Y., and Nakayama, K. (2019). Requirement of IFT-B–BBSome complex interaction in export of GPR161 from cilia. Biol. Open *8*, bio043786.

Nozaki, S., Katoh, Y., Terada, M., Michisaka, S., Funabashi, T., Takahashi, S., Kontani, K., and Nakayama, K. (2017). Regulation of ciliary retrograde protein trafficking by the Joubert syndrome proteins ARL13B and INPP5E. J. Cell Sci. *130*, 563-576.

Takei, R., Katoh, Y., and Nakayama, K. (2018). Robust interaction of IFT70 with IFT52–IFT88 in the IFT-B complex is required for ciliogenesis. *Biol. Open 7*, bio033241.